Human Molecular Genetics, 2004, Vol. 13, No. 24 **3029–3043**
doi:10.1093/hmg/ddh331
Advance Access published on October 20, 2004

Prediction of sensitivity of advanced non-small cell lung cancers to gefitinib (Iressa, ZD1839)

Soji Kakiuchi[1,3], Yataro Daigo[1], Nobuhisa Ishikawa[1], Chiyuki Furukawa[1], Tatsuhiko Tsunoda[2], Seiji Yano[3], Kazuhiko Nakagawa[4], Takashi Tsuruo[6], Nobuoki Kohno[5], Masahiro Fukuoka[4], Saburo Sone[3] and Yusuke Nakamura[1,*]

[1]Laboratory of Molecular Medicine, Human Genome Center, Institute of Medical Science, The University of Tokyo, Minato-ku, Tokyo 108-8639, Japan, [2]Laboratory for Medical Informatics, SNP Research Center, Riken (Institute of Physical and Chemical Research), Yokohama-City, Kanagawa 230-0045, Japan, [3]Department of Internal Medicine and Molecular Therapeutics, The University of Tokushima School of Medicine, Tokushima-City, Tokushima 770-8503, Japan, [4]Department of Medical Oncology, Kinki University School of Medicine, Osaka-Sayama-City, Osaka 589-8511, Japan, [5]Department of Molecular and Internal Medicine, Graduate School of Biomedical Sciences, Hiroshima University, Hiroshima-City, Hiroshima 734-8551, Japan and [6]Laboratory of Cell Growth and Regulation, Institute of Molecular and Cellular Biosciences, The University of Tokyo, Bunkyo-ku, Tokyo 113-0032, Japan

Received June 2, 2004; Revised and Accepted October 11, 2004

Gefitinib (Iressa, ZD1839), an inhibitor of epidermal growth factor receptor-tyrosine kinase, has shown potent anti-tumor effects and improved symptoms and quality-of-life of a subset of patients with advanced non-small cell lung cancer (NSCLC). However, a large portion of the patients showed no effect to this agent. To establish a method to predict the response of NSCLC patients to gefitinib, we used a genome-wide cDNA microarray to analyze 33 biopsy samples of advanced NSCLC from patients who had been treated with an identical protocol of second to seventh line gefitinib monotherapy. We identified 51 genes whose expression differed significantly between seven responders and 10 non-responders to the drug. We selected the 12 genes that showed the most significant differences to establish a numerical scoring system (GRS, gefitinib response score), for predicting response to gefitinib treatment. The GRS system clearly separated the two groups without any overlap, and accurately predicted responses to the drug in 16 additional NSCLC cases. The system was further validated by the semi-quantitative RT–PCR, immunohistochemistry and ELISA for serological test. Moreover, we proved that the anti-apoptotic activity of amphiregulin, a protein that was significantly over-expressed in non-responders but undetectable in responders, leads to resistance of NSCLC cells to gefitinib *in vitro*. Our results suggested that sensitivity of a given NSCLC to gefitinib can be predicted according to expression levels of a defined set of genes that may biologically affect drug sensitivity and survival of lung cancer cells. Our scoring system might eventually lead to achievement of personalized therapy for NSCLC patients.

INTRODUCTION

Lung cancer, the leading cause of cancer death worldwide, is a major health problem in many countries. Chemotherapy is the mainstay for treatment of this disease; surgery is rarely indicated because by the time of diagnosis the majority of lung tumors have reached locally advanced stage III (44%) or metastatic stage IV (32%) (1). Nevertheless, a large meta-analysis revealed that platinum-based chemotherapy prolongs for only about 6 weeks the median survival time of patients with advanced non-small cell lung cancer (NSCLC), compared with the best supportive care (2). Within the last decade, a number of new cytotoxic agents such as paclitaxel, docetaxel, gemcitabine and vinorelbine have emerged to offer

*To whom correspondence should be addressed at: Laboratory of Molecular Medicine, Human Genome Center, Institute of Medical Science, The University of Tokyo, 4-6-1 Shirokanedai, Minato-ku, Tokyo 108-8639, Japan. Tel: +81 354495372; Fax: +81 354495433; Email: yusuke@ims.u-tokyo.ac.jp

multiple choices for patients with advanced lung cancer. However, each of those regimens confers only a modest survival benefit compared with cisplatin-based therapies (3,4). To overcome these limitations, new therapeutic strategies that rely on agents designed to target specific tumor-associated molecules are under development (5,6).

Gefitinib (Iressa, ZD1839) is an orally administered inhibitor of epidermal growth factor receptor-tyrosine kinase (EGFR-TK), an enzyme involved in certain signaling pathways that drive proliferation, invasion and survival of cancer cells (7). Gefitinib has shown potent anti-tumor effects and brought about rapid improvements in NSCLC-related symptoms and quality of life among some patients with advanced NSCLC, who had not responded to platinum-based chemotherapy. In a randomized, double-blind phase II monotherapy trial (the IDEAL 1 trial), the use of gefitinib as a second or third line of chemotherapy achieved tumor-response rates of 18.4% (95% CI: 11.0–25.9%) for advanced NSCLCs; in the IDEAL 2 trial, this drug as the third or fourth line of chemotherapy achieved 11.8% (95% CI: 6.2–19.7%) tumor response (8–10). Moreover, in these trials the drug achieved high rates of disease control (54.4% in IDEAL 1, 42.2% in IDEAL 2) and overall improvement in symptoms (40.3% in IDEAL 1, 43.1% in IDEAL 2). The results were promising when compared with responses to conventional cytotoxic agents, but about half of the patients enrolled in these studies showed no improvement in symptoms and in some cases the medication caused serious adverse effects, including life threatening ones such as interstitial pneumonia (11). The figures do indicate considerable potential for improving prognosis and quality of life for many patients with advanced NSCLC, if we could match treatments to individual cases by using this type of drug more effectively. One approach to that goal is to identify 'cancer profiles' of individual NSCLCs and determine in advance which tumors are likely to respond to gefitinib.

In the study reported here, we applied a cDNA microarray system representing 27 648 genes to select a defined set of genes that could predict responsiveness of advanced NSCLCs to gefitinib. Statistical analysis of expression profiles in 17 clinical samples identified dozens of genes that were differentially expressed between gefitinib-responders and non-responders. A gefitinib-response scoring (GRS) system based on expression patterns of a selected set of those genes successfully predicted the response to gefitinib therapy among additional 16 NSCLC samples. The data was further validated with semi-quantitative RT–PCR, immunohistochemistry and ELISA, implying possible application of our system to practical clinical tests. A gefitinib-sensitivity assay *in vitro* brought to light at least one biological mechanism of gefinitib-resistance of NSCLC cells, i.e. induction of resistance by amphiregulin (AREG). This protein was significantly up-regulated in non-responders, but was not expressed in responders.

RESULTS

Response to gefitinib treatment

Of the 53 patients enrolled in this trial, 46 had tumors diagnosed as adenocarcinomas (86.8%), five were squamous-cell carcinomas (9.4%), two were large-cell carcinomas (3.8%). Fifteen patients achieved a partial response (PR) and nobody revealed a complete response (CR); 17 patients were classified as stable disease (SD) and 19 as progressive disease (PD). No clinical-response data were available for two of the patients. The tumor-response rate (CR + PR/CR + PR + SD + PD) for this treatment was 29.4%, and the disease control rate (CR + PR + SD/CR + PR + SD + PD) was 62.8% (Table 1).

Table 1. Summary of baseline patient characteristics

Characteristics	Percentage (%)	Number of patients
Sex		
Male	58.5	31
Female	41.5	22
Age		
Median	59	
Range	35–80	
Histology		
Adenocarcinoma	86.8	46
Squamous-cell carcinoma	9.4	5
Large-cell carcinoma	3.8	2
Stage		
IIIA	1.9	1
IIIB	7.5	4
IV	90.6	48
Performance status		
0	26.4	14
1	60.4	32
2	13.2	7
Number of prior regimen		
1	24.5	13
2	35.9	19
3	28.3	15
4	0	0
5	7.5	4
6	3.8	2
Response to gefitinib therapy		
CR	0	0
PR	28.3	15
SD	32.1	17
PD	35.8	19
Unknown	3.8	2
Tumor response rate (CR + PR/CR + PR + SD + PD)	29.4	15
Disease control rate (CR + PR + SD/CR + PR + SD + PD)	62.8	32

Tumor samples were collected from 43 patients. Samples from 32 of those 43 contained sufficient numbers of cancer cells for analysis of expression profiles on our cDNA microarray. The numbers of samples that were judged to be suitable for further microarray analysis were 8 for PR, 7 for SD and 13 for PD (Table 2 and Fig. 1). Of the 28 samples, 17 were analyzed as learning cases (seven for PR and 10 for PD) and 11 were test cases (one for PR, three for PD and seven for SD) for establishing a predictive scoring system for the efficacy of gefitinib treatment. For further validation of the prediction system, another blinded set of samples from five newly

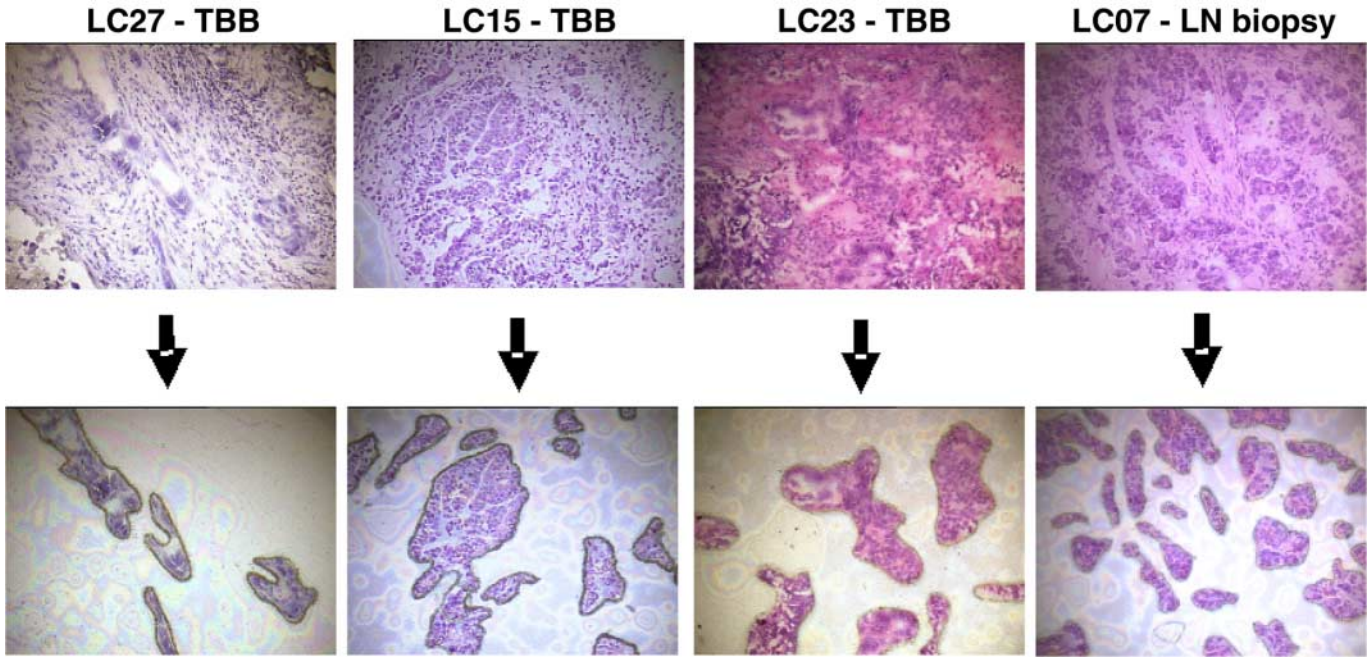

Figure 1. Images illustrating laser-microbeam microdissection of four representative lung adenocarcinomas. The upper row shows the samples before dissection; the lower row, dissected cancer cells (hematoxylin and eosin stain 100×). TBB indicates transbronchial biopsy; LN, lymph-node.

enrolled test-cases (four for PD and one for SD) were obtained and added finally to the initial 11 test cases.

Expression of EGFR and AKT

To determine the status of EGFR and AKT, a downstream effector molecule of EGFR in tumor tissue samples for microarray analysis, we carried out immunohistochemical staining with anti-EGFR, anti-phospho EGFR (p-EGFR), anti-AKT and anti-phospho AKT (p-AKT) antibodies. As shown in Table 7, high levels of EGFR, p-EGFR, AKT and p-AKT protein expression was detected in most NSCLC samples examined, but no correlation between any of these protein expression and sensitivity to gefitinib was observed ($P = 0.999$, 0.622, 0.999 and 0.546, respectively, Fisher's exact test).

Identification of genes associated with sensitivity to gefitinib

We attempted to extract genes that were differentially expressed between tumors from seven patients in the PR group (defined as responders) and those from 10 patients in the PD group (defined as non-responders) by comparing expression levels of 27 648 genes (Tables 2 and 3).

We carried out a random permutation test to distinguish between the two subclasses defined by tumor response, and identified 51 genes whose permutational *P*-values were less than 0.001 (Table 4). Expression levels of 40 genes were higher, and those of the other 11 were lower, in the non-responders.

Table 2. Number of cases suitable for analysis and their best overall responses

Number of cases	Best overall response				
	PR	SD	PD	Unknown	Total
All cases enrolled	15	17	19	2	53
Cases that consented to the study	15	14	13	1	43
Cases suitable for analysis	8	10	13	1	32
Learning cases[a]	7	0	10	0	17
Test cases[a,b]	1	7	3	0	11

[a]Learning cases were used for developing the GRS, whereas test cases were used for validation.
[b]Another blinded set of samples from five newly enrolled cases were also added to the tests later.

Establishment of a predictive scoring system for the efficacy of gefitinib treatment

On the basis of the expression profiles of the 51 genes selected, we tried to establish a predictive scoring system for the efficacy of gefitinib treatment. Prediction scores, termed GRS, were calculated according to procedures described previously (see Materials and Methods). To determine the number of candidates that provided the best separation of the two groups, we ranked the 51 genes on the basis of the significance of their permutational *P*-values and calculated prediction scores by the leave-one-out test, in decrements of one starting from the bottom of the rank-ordered list (51, 50, 49, 48, etc.). We calculated a classification score (CS), a standard we had previously defined for evaluation of the ability to discriminate two classes, for each set of genes.

Table 3. Clinicopathological features of patients

Case no.[a]	Sex	Age	Histology type[b]	T	N	M	Stage classification[c]	Number of previous chemotherapy	EGFR stained tumour cell (%)	Plasma gefitinib concentration (ng/ml)	Response to gefitinib[d] 1st month	2nd month	3rd month	4th month	Best overall response[e]	Use for prediction[f]	GRS[g]
LC01	Female	36	ADC	1	0	1	IV	1		258.9	PR	PR	PR	PR	PR	Learning	100
LC02	Male	64	ADC	2	3	1	IV	3	80	140.3	PR	PR	PR	PR	PR	Learning	100
LC03	Female	54	ADC	2	0	1	IV	3	80	167.0	PR	PR	PR	PR	PR	Learning	100
LC04	Female	75	ADC	2	1	1	IV	1	20	169.7	PR	PR	PR	PR	PR	Learning	100
LC05	Female	73	ADC	0	2	1	IV	5	30	300.6	PR	PR	PR	PR	PR	Learning	100
LC06	Female	75	ADC	4	1	1	IV	3		874.0	SD	PR	PR	PR	PR	Learning	100
LC07	Female	70	ADC	2	1	1	IV	3	80	460.8	SD	PR	PR	PR	PR	Learning	100
LC08	Female	47	ADC	4	3	1	IV	2	95	306.5	PR	PR	PR	PR	PR	Test	54.8
Mean (range)		62 (36–75)						2.6 (1–5)	64 (20–95)	334.7 (140.3–874.0)							
LC09	Female	63	ADC	4	0	1	IV	3	90	743.4	SD	SD	SD	SD	SD	Test	61.6
LC10	Male	56	ADC	2	0	1	IV	6	70	511.8	SD	SD	SD	SD	SD	Test	−9.8
LC11	Male	67	ADC	4	0	1	IV	2	0	631.3	SD	SD	SD	SD	SD	Test	−5.3
LC12	Male	53	ADC	4	3	1	IV	2		306.1	SD	SD	SD	PD	SD	Test	−23.8
LC13	Female	56	ADC	4	2	0	IIIB	2	40	364.8	SD	SD	PD		SD	Test	−58.5
LC14	Female	62	ADC	4	2	1	IV	3	60	322.4	SD	SD	PD		SD	Test	−83
LC15	Male	61	ADC	0	0	1	IV	5	60	278.9	SD	SD	PD		SD	Test	−40.5
Mean (range)		60 (53–67)						3.3 (2–6)	53 (0–90)	451.2 (278.9–631.3)							
LC16	Male	42	ADC	4	3	1	IV	5	90	212.6	SD	PD			PD	Learning	−63.9
LC17	Female	54	ADC	2	3	1	IV	2	50	320.6	SD	PD			PD	Learning	−86
LC18	Female	61	ADC	1	3	0	IIIB	2		229.3	SD	PD			PD	Learning	−67.8
LC19	Male	59	ADC	0	2	1	IV	2	30	150.7	SD	PD			PD	Learning	−57.1
LC20	Male	65	ADC	0	3	1	IV	3		167.8	SD	PD			PD	Learning	−59.1
LC21	Male	55	ADC	4	3	1	IV	3	80		PD				PD	Learning	−73.1
LC22	Male	80	ADC	4	3	1	IV	2	80		PD				PD	Learning	−55.5
LC23	Male	35	ADC	4	0	1	IV	5			PD				PD	Learning	−100
LC24	Male	57	ADC	4	3	1	IV	1	0		PD				PD	Learning	−46.7
LC25	Female	65	ADC	2	0	1	IV	1		356.3	PD				PD	Learning	−86.1
LC26	Male	64	SCC	3	3	1	IV	2		405.6	SD	PD			PD	Test	-67.7
LC27	Female	65	ADC	4	2	1	IV	1			PD				PD	Test	−69.4
LC28	Male	74	ADC	2	1	1	IV	1	10		PD				PD	Test	−64.8
Mean (range)		60 (35–80)						2.3 (1–5)	49 (0–90)	263.2 (150.7–405.6)							

[a]For further validation of the GRS, another blinded set of samples from five newly enrolled cases (four PD and one SD) were also added to these 28 cases later.
[b]ADC, adenocarcinoma; SCC, squamous-cell carcinoma.
[c]TNM clinical classification and stage grouping were assessed based on the UICC/WHO classification.
[d]Objective tumor response to gefitinib was assessed every 4 weeks after the start of treatment using UICC/WHO Criteria. PR, partial response; SD, stable disease; PD, progressive disease.
[e]Overall best response was evaluated based on the definitions as mentioned in Materials and Methods.
[f]Learning, samples used for developing the GRS; Test, samples used for validation of the GRS.
[g]GRS, gefitinib response score determined by prediction system.

Table 4. List of 51 candidate genes for discriminating responder (PR) from non-responder (PD) to gefitinib[a]

Rank order	GenBank accession no.	Symbol	Gene name	Predominantly expressed class	Permutational *P*-value	Median-fold difference (log 2)
1	NM_024829	*FLJ22662*	Hypothetical protein FLJ22662	PD	8.1×10^{-12}	2.0
2	BC009799	*AREG*	Amphiregulin (schwannoma-derived growth factor)	PD	9.3×10^{-12}	8.0
3	NM_014325	*CORO1C*	Coronin, actin binding protein, 1C	PD	2.3×10^{-10}	4.6
4	BC010488	*AVEN*	Apoptosis, caspase activation inhibitor	PD	4.2×10^{-10}	4.3
5	NM_004090	*DUSP3*	Dual specificity phosphatase 3 (vaccinia virus phosphatase VH1-related)	PD	9.4×10^{-10}	4.4
6	AI026836	*DJ473B4*	Hypothetical protein dJ473B4	PD	1.7×10^{-9}	8.0
7	BU500509	*PHLDA2*	Pleckstrin homology-like domain, family A, member 2	PD	1.8×10^{-9}	8.0
8	NM_016090	*RBM7*	RNA binding motif protein 7	PD	1.8×10^{-8}	2.9
9	BX092512		EST	PD	7.7×10^{-8}	3.0
10	AI436027	*OSMR*	Oncostatin M receptor	PD	1.1×10^{-7}	3.7
11	AI971137	*GCLC*	Glutamate–cysteine ligase, catalytic subunit	PD	1.2×10^{-7}	3.9
12	BQ024877	*COL4A3BP*	Collagen, type IV, alpha 3 (Goodpasture antigen) binding protein	PD	2.0×10^{-7}	3.6
13	U52522	*ARFIP2*	ADP-ribosylation factor interacting protein 2 (arfaptin 2)	PD	2.6×10^{-7}	2.8
14	BM996053	*C10orf9*	Chromosome 10 open reading frame 9	PD	4.2×10^{-7}	2.5
15	AK025452	*NIP30*	NEFA-interacting nuclear protein NIP30	PD	5.1×10^{-7}	3.7
16	N52048	*KIAA0776*	KIAA0776 protein	PD	5.4×10^{-7}	7.2
17	AA507009	*SLC35F2*	Solute carrier family 35, member F2	PD	6.0×10^{-7}	5.8
18	AA226243	*GAMLG*	Calcium modulating ligand	PD	6.8×10^{-7}	5.0
19	AF005888	*NOC4*	Neighbor of COX4	PD	1.1×10^{-6}	4.0
20	AF012281	*PDZK1*	PDZ domain containing 1	PD	1.3×10^{-6}	4.5
21	AI188190	*DIS3*	Mitotic control protein dis3 homolog	PD	1.7×10^{-6}	3.8
22	BC001535	*CGI-48*	CGI-48 protein	PD	2.0×10^{-6}	3.5
23	NM_007007	*CPSF6*	Cleavage and polyadenylation specific factor 6, 68 kDa	PD	2.2×10^{-6}	3.4
24	NM_002254	*KIF3C*	Kinesin family member 3C	PD	2.2×10^{-6}	3.5
25	BQ135232	*CD9*	CD9 antigen (p24)	PD	2.2×10^{-6}	1.7
26	BC051322	*LRRC8*	Leucine rich repeat containing 8	PD	2.5×10^{-6}	3.4
27	BC038504	*SNF1LK*	SNF1-like kinase	PD	2.6×10^{-6}	2.8
28	U78556	*CRA*	Cisplatin resistance associated	PD	2.7×10^{-6}	3.7
29	BC035625	*EGR2*	Early growth response 2 (Krox-20 homolog, *Drosophila*)	PD	3.4×10^{-6}	3.0
30	X52426	*KRT13*	Keratin 13	PD	1.9×10^{-5}	3.4
31	NM_005504	*BCAT1*	Branched chain aminotransferase 1, cytosolic	PD	2.3×10^{-5}	1.7
32	NM_006643	*SDCCAG3*	Serologically defined colon cancer antigen 3	PR	2.6×10^{-5}	3.7
33	AA464095	*PIGK*	Phosphatidylinositol glycan, class K	PD	3.2×10^{-5}	1.1
34	AA961188	*MRPS9*	Mitochondrial ribosomal protein S9	PD	9.8×10^{-5}	2.3
35	NM_018123	*ASPM*	asp (abnormal spindle)-like, microcephaly associated (*Drosophila*)	PR	2.3×10^{-4}	2.8
36	NM_022735	*ACBD3*	acyl-Coenzyme A binding domain containing 3	PD	2.4×10^{-4}	3.8
37	AA160544	*ZNF325*	Zinc finger protein 325	PR	2.7×10^{-4}	4.5
38	AK057653	*LOC285513*	Hypothetical protein LOC285513	PD	2.7×10^{-4}	3.8
39	NM_003310	*TSSC1*	Tumor suppressing subtransferable candidate 1	PD	2.9×10^{-4}	4.7
40	BC007451	*XAB1*	XPA binding protein 1	PD	3.0×10^{-4}	1.3
41	BC035467	*HNLF*	Putative NFkB activating protein HNLF	PR	3.5×10^{-4}	1.1
42	CK004097	*EIF4EBP2*	Eukaryotic translation initiation factor 4E binding protein 2	PR	3.6×10^{-4}	1.4
43	NM_144683	*MGC23280*	Hypothetical protein MGC23280	PR	4.2×10^{-4}	2.3
44	NM_004600	*SSA2*	Sjogren syndrome antigen A2 (60 kDa, ribonucleoprotein autoantigen SS-A/Ro)	PR	4.2×10^{-4}	1.2
45	NM_002730	*PRKACA*	Protein kinase, cAMP-dependent, catalytic, alpha	PR	5.0×10^{-4}	1.2
46	NM_005102	*FEZ2*	Fasciculation and elongation protein zeta 2 (zygin II)	PD	6.1×10^{-4}	3.3
47	NM_005839	*SRRM1*	Serine/arginine repetitive matrix 1	PR	7.0×10^{-4}	1.4
48	NM_006207	*PDGFRL*	Platelet-derived growth factor receptor-like	PD	7.0×10^{-4}	2.4
49	AI096936	*SNX13*	Sorting nexin 13	PR	8.4×10^{-4}	1.6
50	NM_014785	*KIAA0258*	KIAA0258 gene product	PD	8.9×10^{-4}	2.5
51	BF973104	*TOM7*	Homolog of Tom7 (*S. cerevisiae*)	PR	1.0×10^{-3}	1.5

[a]The top 12 and 51 gene sets were listed as the rank-order of permutational *P*-values that were < 0.001.

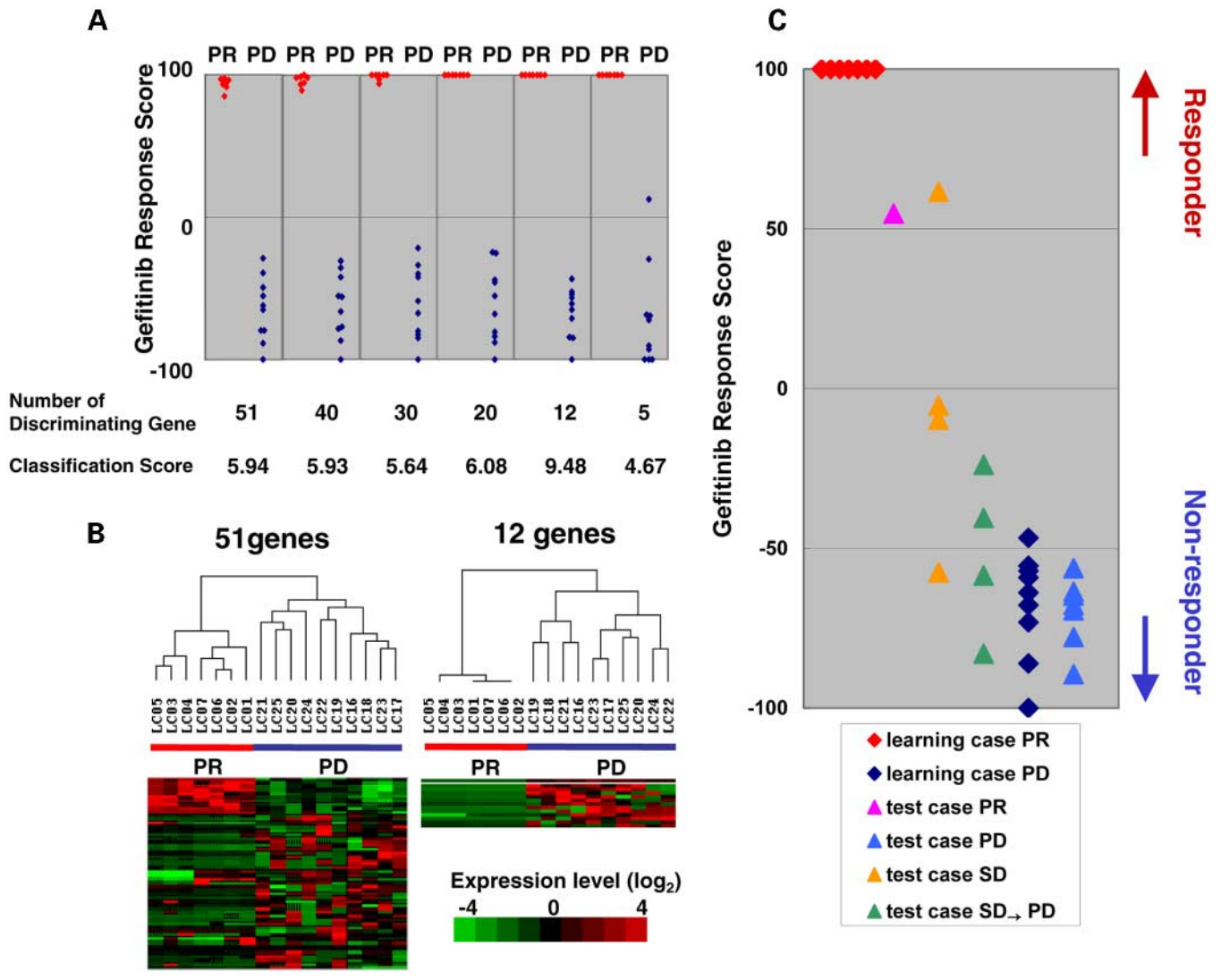

Figure 2. Establishing a scoring system to predict the efficacy of gefitinib treatment. (**A**) Different prediction scores appear when the number of discriminating genes is changed. The number of the discriminating gene sets (5–51) corresponds to the number of selected genes from the top of the rank-ordered list in Table 4. A larger value of classification score (CS) indicates better separation of the two groups. (**B**) Hierarchical clustering of 17 'learning' cases using 51 candidate genes for gefitinib sensitivity (left), and 12 prediction genes that were finally selected for the GRS (right). The dendrograms represent similarities in expression patterns among individual cases; longer branches indicate greater differences. The two groups were most clearly separated by the 12-gene set. (**C**) Schematic distinction of responder, non-responder and 'test cases' verified on the basis of the GRS. Red diamonds denote prediction scores for learning PR cases and blue diamonds represent learning PD cases. A pink triangle indicates a test PR case that had not been used for establishing GRS and blue triangles indicate test PD cases. Yellow triangles indicate test SD cases that kept the SD status throughout the 4 month observation period and green triangles indicate test cases once judged as SD at a certain time point of the study but showed progression of the disease within 3 or 4 months after the start of treatment.

As shown in Figure 2A, we obtained different prediction scores when the number of discriminating genes was changed. We obtained the best CS, meaning the best separation of responders from non-responders, when we calculated the scores using only the 12 top-ranked genes in our candidate list.

Hierarchical clustering analyses using all 51 genes, or only the top 12, classified all 17 cases into one of two groups according to the response to gefitinib (Fig. 2B). The two groups were most clearly separated when we used the top 12 genes for cluster analysis. Finally, we established a numerical drug-response-scoring algorithm that might be clinically applicable for predicting sensitivity of an individual NSCLC to gefitinib, on the basis of expression levels of the 12 selected genes.

To validate this prediction system, we investigated eight additional ('test') NSCLC cases (one for PR and seven for PD) that were completely independent of the 17 'learning' cases used for establishing the system. We examined gene-expression profiles in each of those samples and then calculated GRS on the basis of the expression levels of the 12 discriminating genes. As shown in Figure 2C, scores obtained by the GRS system were concordant with the clinical responses to gefitinib in all eight 'test' cases.

Table 5. Correlation of cDNA microarray data with RT–PCR

Rank order	Gene symbol	Spearman rank correlation ρ	*P*-value
1	*FLJ22662*	0.69	0.02
2	*AREG*	0.53	0.08
3	*CORO1C*	0.35	0.24
4	*AVEN*	0.63	0.04
5	*DUSP3*	0.63	0.04
6	*DJ473B4*	0.45	0.14
7	*PHLDA2*	0.84	0.01
8	*RBM7*	0.83	0.01
9	*EST(BX092512)*	0.63	0.04
10	*OSMR*	0.67	0.03
11	*GCLC*	0.46	0.13
12	*COL4A3BP*	0.27	0.24

Correlations positive for all 12 genes and significantly positive for seven of 12.

Table 6. Result of immunohistochemical staining for prediction markers

	PR	PD
AREG	1/5	5/6
TGFA	2/5	6/6
ADAM9	1/5	4/6
CD9	2/5	5/6
OSMR	2/5	6/6

Table 7. Result of immunohistochemical staining for EGFK and AKT

	PR	PD
EGFR	6/6	6/7
p-EGFR	5/7	5/9
p-AKT	4/5	4/6
AKT	4/6	4/6

GRS values for patients with SD in tumor response

GRS values for the eight test-SD patients were calculated according to the predictive scoring system established earlier. Although the values were widely distributed from −83.0 (predicted as non-responder) to 61.6 (responder), the scores of patients who retained SD status throughout the observation period were likely to be higher than those of patients who had been judged as SD at a certain time-point of the study but showed progression of the disease within 3 or 4 months after the start of treatment (Fig. 2C). Although the GRS system was established on the basis of gene-expression profiles that distinguished between patients with PR and patients with PD (without SD) in tumor response, these results suggested the possibility that the GRS may serve in classifying SD patients into groups according to their response to gefitinib.

Validation of GRS with semi-quantitative RT–PCR analysis

To confirm differential expression of the top 12 predictive genes between PR and PD cases, expression values derived from microarray data were correlated with values from semi-quantitative RT–PCR of RNAs from the same patients (five PR and seven PD) (Table 5 and Fig. 3A). Spearman rank correlations were positive for all of the 12 genes and significantly positive for seven of 12 genes.

Immunohistochemical validation of GRS

To validate differential expression of the predictive protein markers between PR and PD cases, we carried out immunohistochemical staining with five different antibodies for AREG, TGFA, ADAM9, CD9 and OSMR, all of which were known to be involved in the ligand-EGFR signaling and whose permutational *P*-values were < 0.01 (Supplementary Material, Table S1). We first stained paired tumor tissue sections obtained by TBB and lymph-node biopsy from the same patients using these five antibodies. No intra-patient differences on protein expression of these five markers were observed in three different patients (Fig. 3B). We also validated the microarray data with the five markers in 11 NSCLC samples (five for PR and six for PD). The results were consistent with the microarray data (Table 6 and Fig. 3C).

Serum levels of TGFA

To further evaluate the availability of the prediction system in routine clinical situations, we detected TGFA protein which was known to be the ligand for EGFR and whose permutational *P*-values were < 0.01, using ELISA in serum samples from five PR, 10 SD and 20 PD patients that were independently collected for serological test and were not enrolled in microarray analysis. The serum levels of TGFA were 19.0 ± 2.8 pg/ml (mean $\pm$ SE) in PD patients, 13.9 ± 1.9 pg/ml in SD patients and 12.8 ± 1.4 pg/ml in PR patients (Fig. 4). Twelve of 20 serum samples from PD patients were positive for TGFA and all samples from PR patients were negative, when 16.0 pg/ml was used as a cutoff.

In vitro gefitinib treatment and AREG-autocrine assay

AREG, a ligand for EGFR and other ERBB members, was significantly over-expressed in non-responders but not (or hardly) detectable in responders. To investigate whether AREG protein leads to resistance of NSCLCs to gefitinib therapy when it is secreted in an autocrine manner, we performed the following biological analyses. We initially identified expression of AREG mRNA in lung-adenocarcinoma cell lines NCI-H358 and -H522, but not in PC-9, by means of RT–PCR experiments (Fig. 5A). Next, we performed flow-cytometric analysis 72 h after treatment of PC-9 cells with 1.0 μM of gefitinib, and found that gefitinib increased the percentages of nuclei in sub-G_1 (24%) compared with cells with no treatment (6%) (data not shown). This result suggested that gefitinib might induce apoptosis in PC-9 cells.

We then analyzed the viability of PC-9 cells, which are gefitinib-sensitive and do not express *AREG*, after culture in serum-free medium or in serum-free, conditioned medium

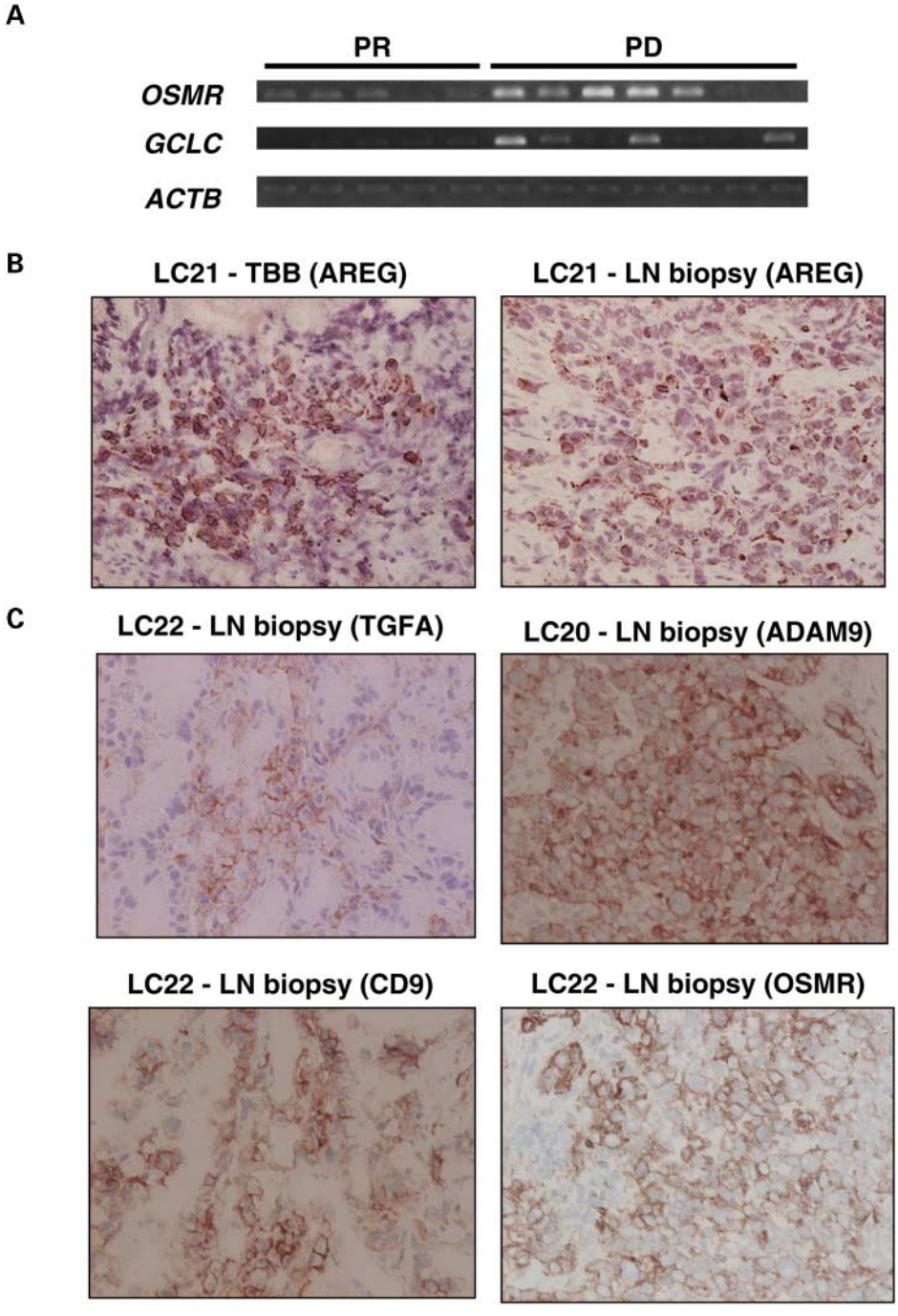

Figure 3. Validation of GRS with semi-quantitative RT–PCR and immunohistochemical analyses. (**A**) Representative image of semi-quantitative RT–PCR analysis of RNAs from the PR and PD groups. *OSMR* and *GCLC* genes were over-expressed in non-responders (PD). The integrity of each cDNA template was controlled through amplification of *ACTB*. (**B**) Immunohistochemical staining of representative samples from fiberscopic transbronchial biopsy (TBB) and lymph-node (LN) biopsy from the same PD-patient (no. LC21), using anti-AREG antibody (×200). (**C**) Immunohistochemical staining of representative samples from PD patients, using antibodies for other four prediction markers (TGFA, ADAM9, CD9 and OSMR) (×200).

obtained from NCI-H358 or -H522 cells grown in the presence or absence of 0.5 or 1.0 μM of gefitinib. As shown in Figure 5B, the viability of PC-9 cells incubated in the serum-free, conditioned medium containing gefitinib was greater than that of PC-9 cells grown in serum-free medium with the same concentrations of gefitinib.

To investigate whether AREG, secreted in an autocrine manner, inhibits apoptosis of NSCLC cells treated with gefitinib, we cultured PC-9 cells in serum-free medium containing recombinant AREG protein at final concentrations of 1–100 ng/ml, in the presence or absence of 1.0 μM gefitinib. The viability of PC-9 cells incubated with both AREG and

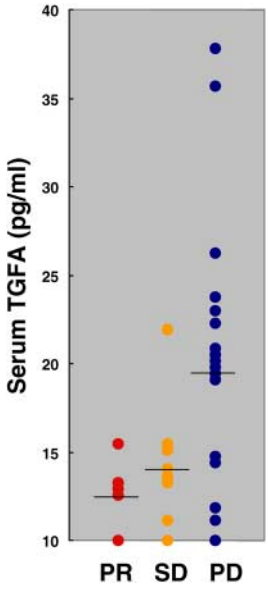

Figure 4. Serologic concentration of TGFA determined by ELISA in five PR, 10 SD and 20 PD adenocarcinoma cases. The averaged serum levels of TGFA were shown as black bars: 19.0 ± 2.8 pg/ml (mean ± SE) in PD patients, 13.9 ± 1.9 pg/ml in SD patients, and 12.8 ± 1.4 pg/ml in PR patients.

1.0 μM gefitinib was increased when compared with cells incubated with 1.0 μM gefitinib only, in an AREG dose dependent manner (Fig. 5C). On the other hand, recombinant AREG alone had no effect on the viability of PC-9 cells (Fig. 5C). This observation appeared to indicate that AREG inhibits the apoptosis induced by gefitinib, but does not in itself affect cell viability.

DISCUSSION

A large body of evidence supports the view that molecules in the EGFR autocrine pathway are involved in a number of processes important to cancer formation and progression, including cell proliferation, angiogenesis and metastatic spread (5). Therapeutic blockade of specific signaling, therefore, could be a promising strategy for cancer treatment. Gefitinib, a synthetic anilinoquinazoline, inhibits the tyrosine kinase activity of EGFR by competing with adenosine triphosphate for a binding site on the intracellular domain of the receptor (7). In phase II trials (IDEAL 1 and IDEAL 2), use of gefitinib as a second, third or fourth line monotherapy for advanced NSCLC achieved tumor-response rates of nearly 20% (8–10), which were superior to those achieved with conventional cytotoxic agents. Multivariate analysis of patients in the IDEAL 1 study suggested that the response rate in females might be higher than in males, and higher in patients with adenocarcinomas than in patients with squamous-cell carcinomas (odds ratios 2.7 and 3.5, respectively) (9). Recent study suggested that individuals in whom gefitinib is efficacious are more likely to have adenocarcinomas of the bronchioloalveolar subtype and to be never smokers (odds ratios 13.5 and 4.2, respectively) (12). The higher tumor-response rate (29.4%) documented in the clinical trial reported here might reflect a higher proportion of patients with adenocarcinoma (46 adenocarcinomas, five squamous-cell carcinomas and two large-cell carcinomas) than has been the case in other studies. The clinicopathological determinants of gefitinib sensitivity, including bronchioloalveolar carcinoma (BAC) features, are predictive to a certain extent (9,10,12,13); however, previous reports and our observations obviously suggest that no factors can perfectly predict the response of NSCLC to gefitinib treatment. It was also reported quite recently that somatic mutations of *EGFR* may predict sensitivity to gefitinib and mutant EGFRs selectively may activate AKT and STAT signaling *in vitro*, which transduce anti-apoptotic pathways (14–16); however, our mutational search proved that there is no significant correlation between the *EGFR* mutations and disease control effect of gefitinib therapy (PR + SD versus PD) (data not shown). Moreover, there is no evidence of correlation between response to gefitinib treatment and AKT/p-AKT protein level. We also did not identify transcriptional activation of the components of AKT/STAT signaling in the list of our prediction genes (top 132 genes; $P < 0.01$; Supplementary Material, Table S1). This result independently confirms no correlation between sensitivity to gefitinib and activation of AKT/STAT signaling. Therefore, novel methods to precisely discriminate responders from non-responders in advance could allow a more focused use of gefitinib in clinical settings.

By statistical analysis of gene-expression profiles of advanced NSCLCs obtained on cDNA microarrays, we identified dozens of genes associated with sensitivity to gefitinib. We introduced a prediction-scoring system based on expression of the 12 genes that had shown the most significant differences in expression levels between responder (PR) and non-responder (PD) groups. This set of genes was selected from expression profiles of lung adenocarcinomas; however, the GRS system successfully classified all eight of our 'test' PR and PD cases in accord with their clinical responses to gefitinib, and one of them was a squamous-cell carcinoma. Moreover, this system was likely to separate intermediate tumor responses (SD) into two groups, one representing patients who succeeded in maintaining the tumor-static effect for a long period and the other representing patients who failed to do so, although validation of the system in larger prospective trial is warranted.

In practical terms, we need to predict the chemosensitivity of individual tumors using the minimally invasive techniques available at every hospital, because patients with advanced NSCLCs are rarely candidates for surgical resection of their tumors. Therefore, we have tried to establish a prediction system that requires only the amount of cancerous tissue that can be obtained by, for example, flexible bronchofiberscopy. By verifying individual steps of the method, we were able to precisely profile gene expression in biopsy specimens as small as 1 mm. Relevant microarray results were confirmed by semi-quantitative RT–PCR for 12 genes that showed the most significant differences to establish a GRS system. Furthermore, we validated the effectiveness of antibodies for five different biomarkers (AREG, TGFA, ADAM9, CD9 and OSMR), all of which were reported to be involved in the ligand-EGFR signaling, for discriminating potential responders from non-responders, in both TBB and lymph-node

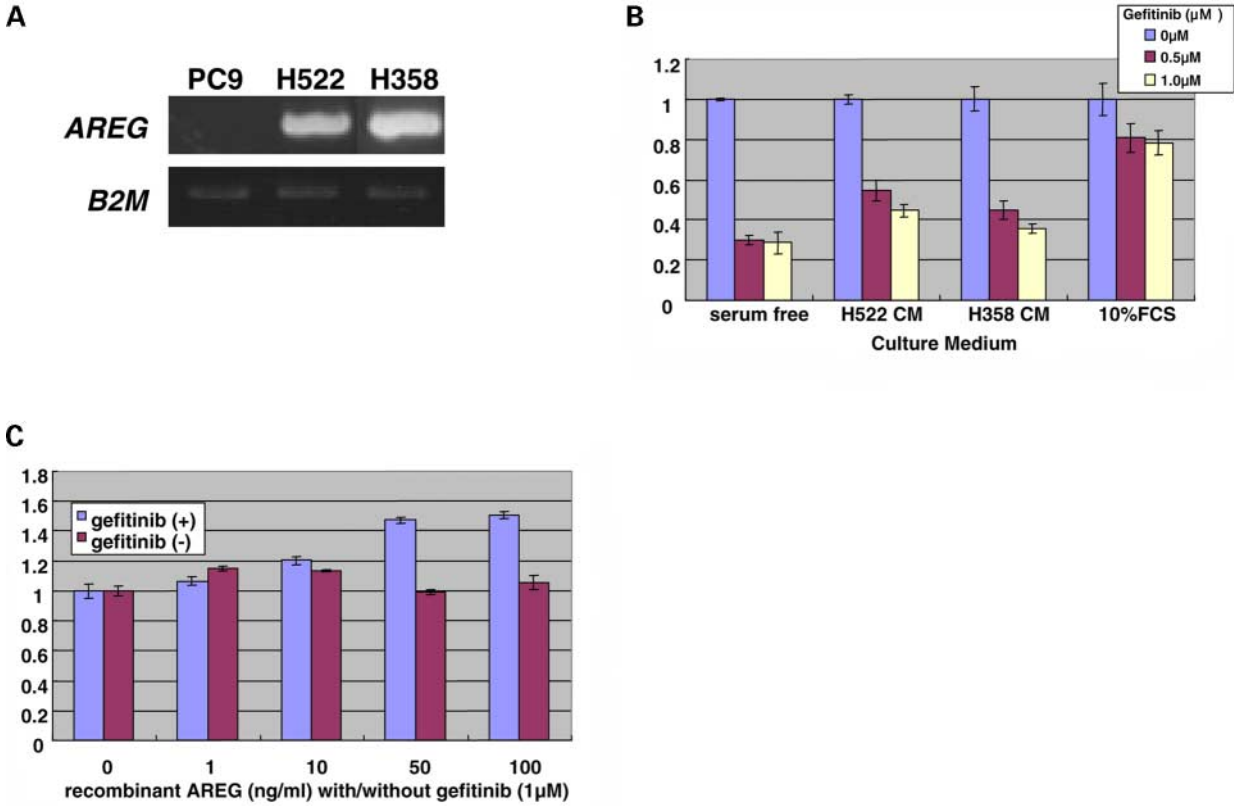

Figure 5. Anti-apoptotic effect of secreted AREG on gefitinib-sensitive PC-9 cells. (**A**) Expression of *AREG* transcript examined by semi-quantitative RT–PCR in lung adenocarcinoma cell lines PC-9, NCI-H358 and -H522. (**B**) PC-9 cells cultured in medium supplemented with 10% FCS, in serum-free medium or in serum-free conditioned medium (CM) obtained from cultures of NCI-H358 or -H522 cells. Each medium was replaced once with the same medium at the 48 h time point; 72 h after adding gefitinib at concentrations of 0.5 or 1.0 μM, cell viability was measured by MTT assays. The experiments were done in triplicate. The *y*-axis indicates the relative MTT value (MTT in the presence of 0.5 or 1.0 μM gefitinib/MTT in the absence of gefitinib) of the cells incubated in different media. (**C**) Effect of AREG, secreted in an autocrine manner, on the resistance of NSCLC cells to gefitinib. At the start of culture, PC-9 cells were inoculated into medium containing 1.0 μM gefitinib and recombinant AREG protein (final concentrations of 1–100 ng/ml); 72 h later, cell viability was measured by triplicate MTT assays (blue bars). The *y*-axis indicates the relative MTT values (MTT at individual concentrations of AREG/MTT without AREG) of the cells. Effect of AREG on the viability of NSCLC cells in the absence of 1.0 μM gefitinib was also studied. Individual PC-9 cells were added to medium containing recombinant AREG protein but no gefitinib; 72 h later, viability was measured by triplicate MTT assays (red bars).

biopsy samples. These five markers are cell-surface or secretory proteins and should have significant advantages for development of a novel serum maker for predicting response to gefitinib treatment, because they are presented either on the cell surface or within the extracellular space, and/or in serum, making them easily accessible as molecular markers. In fact, we were able to detect serum TGFA proteins in lung-adenocarcinoma patients by ELISA. Further evaluation of these markers for clinical use is necessary; however, the limited number of genes required for prediction should eventually enable laboratories to diagnose in advance the efficacy of gefitinib treatment for an NSCLC patient, using routine procedures such as serological examinations of blood, PCR experiments or immunohistochemical analysis of biopsy specimens.

To our knowledge, this is the first report about gene-expression profiles of unresectable 'advanced' lung cancers, although profiles of surgically resected specimens of 'early' lung cancers have been reported (17,18). However, ~70% of tumors in patients diagnosed with NCSLC are already locally advanced or metastatic, which generally renders them resistant to conventional therapeutic modalities. Therefore, the genes listed here should be useful for disclosing molecular mechanisms of lung cancer progression and may be potential targets for drug development.

Gefitinib was developed as a 'selective' inhibitor of EGFR-TK; however, no clear association between the level of EGFR activation and response to gefitinib has been found *in vitro* or *in vivo* (7,19). In clinical trials, gefitinib has been more effective against adenocarcinomas than against squamous-cell carcinomas (9,10), although over-expression of EGFR is less frequent in adenocarcinomas (20). Therefore, it is important to identify which individual tumors are good targets for this treatment. In our analysis using clinical samples, the difference in EGFR (p-EGFR)/AKT (p-AKT) protein expression and *EGFR* mutation between treatment-sensitive patients and resistant patients were not significant. On the other hand, amphiregulin (*AREG*) and transforming growth factor alpha (*TGFA*), both of which encode the ligand for EGFR and other ERBB members, were significantly over-expressed in non-responders but not (or hardly) detectable in responders ($P = 0.0000000000093$ and 0.0095, respectively; Table 4).

The results of this trial support further evaluation of the GRS system in another set of study population with NSCLC patients treated with gefitinib. The prospective trial to evaluate the reliability of several prediction systems including our GRS and controversial tests for EGFR signaling status is in progress in our institute.

The significance of the ligands and the EGFR autocrine loop in growth and survival of lung cancer cells is indisputable (20–22), but the role of AREG in formation and progression of cancers is poorly understood. However, several lines of evidence suggest that over-expression of *AREG* is associated with shortened survival of patients with NSCLC (20). Moreover, anti-apoptotic activity of AREG in human lung-adenocarcinoma cells was reported recently (21). To investigate whether the anti-apoptotic activity of AREG leads to resistance of NSCLC cells to gefitinib therapy, we performed a biological assay using a gefitinib-sensitive but *AREG*-non-expressing NSCLC cell line, PC-9. We found that the anti-tumor activity of gefitinib on PC-9 cells was dramatically decreased by autocrine secretion of AREG. This evidence strongly suggests that although growth factor signaling by the EGFR is markedly complicated at every step because of the multiplicity of ligands, dimerization partners, effectors and downstream pathways (22), AREG might be a principal activator of the ligands–receptor autocrine growth pathway that leads to cancer progression and resistance to gefitinib.

Several elements associated with the EGFR-TK pathway are present on our list of differentially expressed genes. For example, genes encoding dual specificity phosphatase 3 (*DUSP3*), *ADAM9 CD9* and *OSMR* were expressed predominantly in non-responders ($P = 0.00000000094$, 0.01, 0.000022 and 0.0000011, respectively). *DUSP3* gene modulates EGFR signaling by dephosphorylating mitogen activated protein kinase (MAPK), a key mediator of signal transduction (23), and ADAM9 is involved in activation of EGFR signaling by shedding the ectodomain of proHB-EGF (pro Heparin-binding epidermal growth factor-like growth factor) (24). CD9 physically interacts with transmembrane TGFA. CD9 expression strongly decreases the growth factor- and PMA-induced proteolytic conversions of transmembrane to soluble TGFA and strongly enhances the TGFA-induced EGFR activation (25). OSMR is reported to be constitutively associated with ERBB2 in breast cancer cells (26). Although other target molecules for gefitinib have been suggested, our results suggest that EGFR signaling containing these components is at least one of the important processes involved in response to this drug.

Since gefitinib can induce apoptosis of some cancer cells *in vivo*, other molecules with anti-apoptotic activity, as well as AREG, may contribute to a tumor's resistance to the drug. *AVEN* (apoptosis, caspase-activation inhibitor), which was specifically expressed in our non-responders ($P = 0.00000000042$), is known to enhance the anti-apoptotic activity of Bcl-xL and to suppress Apaf-1-mediated caspase activation (27). On the other hand, mechanisms regulating drug transport should also affect drug resistance. *GCLC* (glutamate–cysteine ligase, catalytic subunit), which plays an important role in cellular detoxification of anti-cancer drugs such as cisplatin, etoposide and doxorubicin (28), was over-expressed in our group of non-responders ($P = 0.00000012$). As these genes correlated negatively with responses to chemotherapy in our panel of tumors (i.e. the higher the expression of these genes, the greater the resistance to gefitinib), they might be involved in the mechanism(s) leading to that resistance. It should be noted also that the functions of nearly half of our candidate prediction genes are unknown. Therefore, further investigations will be needed to reveal more clearly the biological events underlying responses of NSCLCs to gefitinib.

CONCLUSION

We identified 51 genes whose expression differed significantly between responders and non-responders to gefitinib among human lung carcinomas, and established a numerical scoring system, based on expression patterns of 12 of those genes, to predict the response of individual tumors to this drug. Although further validation using a larger set of clinical cases will be necessary, the data presented here may yield valuable insights into the molecular events underlying signal-suppressing strategies and provide important information about gefitinib treatment for individual NSCLC patients by testing a set of genes with high predictive values.

MATERIALS AND METHODS

Patients and tissue samples

From December 2001 to November 2003, we carried out a phase II clinical study entitled 'Multi-center trial to explore the dominant biological factors responsible for clinical anti-tumor effect and pharmacokinetics of ZD1839 250 mg daily in patients with advanced non-small-cell lung cancer who have failed previous chemotherapy'. The primary endpoint was to clarify a gene-expression profile that could determine in advance a potential anti-tumor effect of gefitinib. At the beginning of the study, the rationale for the sample size was estimated from that of studies conducted thus far (29,30). Since the response rate for gefitinib was $<20\%$ in the patients of lung cancer (8–10), about 50 patients were supposed to be required to obtain learning cases estimated earlier. Patients whose locally advanced (stage IIIB) or metastasized (stage IV) NSCLCs were resistant to one or more regimens of conventional chemotherapy were enrolled in this trial. Inclusion criteria were (1) age >20 years, (2) performance status (PS) 0–2, (3) adequate liver and kidney function tests. All patients were treated with 250 mg of gefitinib orally once a day at the Tokushima University or Kinki University hospitals in Japan. The treatment was continued until the patient was dropped from the study due to (1) progression of disease, (2) intolerable toxicity, (3) withdrawal of consent.

Objective tumor responses were assessed every 4 weeks after the beginning of treatment, according to criteria outlined by the *Union International Contre le Cancer*/World Health Organization (UICC/WHO). Response categories were as follows: complete response (CR), no residual tumor in any evaluable lesion; partial response (PR), residual tumor with evidence of $\geq 50\%$ decrease under baseline in the sum of all measurable lesions, and no new lesions; progressive disease (PD), residual tumor with evidence of $\geq 25\%$ increase

under baseline in the sum of all measurable lesions, or appearance of new lesions; and stable disease (SD), residual tumor not qualified for CR, PR or PD. All evaluable lesions were measured bi-dimensionally (sum of products of longest diameter and its longest perpendicular of measurable lesions) using the same techniques as baseline, e.g. plain X-ray, CT or MRI.

At the end of 4-month treatment (or withdrawal), the best overall response was evaluated for each patient based on definitions as follows: CR, patients who qualified for CR at two sequential examination points with an interval of at least 28 days between them; PR, patients judged as PR or better at two sequential examination points with an interval of at least 28 days between them; SD, patients who were SD or better at two sequential examination points at least 28 days apart but who did not qualify as CR or PR. The first judgment of an SD case must be done at or after the first tumor assessment point (28 days after randomization); PD, the patients determined as PD at or before the first tumor assessment point (28 days after randomization); unknown, the patient does not qualify for a best response of increased disease, and all objective statuses after baseline (before randomization) and before progression are unknown.

Prior to the gefitinib treatment, tumor specimens were taken by transbronchial (TBB), skin or lymph-node biopsy with written informed consent from each patient. Ethics approval was obtained from the ethics committee of the individual institutes. Biopsy samples were frozen immediately, embedded in TissueTek OCT medium (Sakura, Tokyo, Japan), and stored at -80°C. All samples were examined microscopically, and samples from 28 patients (17 learning and 11 test cases) that contained enough cancer cells for analysis of expression profiles were initially selected for further analysis. For validation of the prediction system, a blinded set of samples from five newly enrolled cases (four PD and one SD) were also added to the 11 test cases. EGFR and AKT protein expression in tumor tissues, and plasma concentration of gefitinib were measured as additional biological factors in this study. Tissue sections from 19 suitable cases were used for assessment of EGFR protein expression as %positive cells with immunohistochemistry (DakoCytomation, Glostrup, Denmark). p-EGFR, AKT and p-AKT positivity were assessed on available tissue sections as absent or positive using individual monoclonal antibodies (Cell Signaling Technology, Inc., Beverly, MA, USA). Clinical and histological information about these patients is summarized in Tables 1–3.

Microdissection

In view of significant differences in the proportions of cancer cells and various types of parenchymal cells that are present from one tumor to another, microdissection is a necessary means of obtaining precise gene-expression profiles on cDNA microarrays. Therefore, we stained 8 μm thick frozen sections with hematoxylin and eosin and collected cancer cells selectively, using the μCUT laser-microbeam microdissection system (Molecular Machines & Industries AG, Glattbrugg, Switzerland) (31). In this system, tissue sections are mounted on a thin supporting polyethylene membrane that will be cut together with the target tissue; a pulsed ultraviolet (UV) narrow-beam-focus laser cuts out cancer cells along a pre-selected track that can be observed on a video screen. The material to be extracted is never directly exposed to the laser but only circumscribed by it; unlike other LMM systems, this one allows recovery of dissected cells to proceed without radiation. Moreover, the membrane protects the tissue on the slide against cross-contamination. Using this system we were able to isolate small areas of tissue rapidly, and to isolate single cells from histological sections (Fig. 1).

RNA extraction and T7-based RNA amplification

Total RNA was extracted from individual microdissected populations of cancer cells using RNAeasy mini kits and RNase-free DNase kits (QIAGEN, Hilden, Germany) according to the manufacturer's protocols. Total RNAs were subjected to T7-based RNA amplification, as described previously (32). Two rounds of amplification yielded 40–200 μg of aRNA (>100 000-fold) from each sample. As a control probe, normal human lung poly(A)$^+$RNA (BD Biosciences Clontech, Palo Alto, CA, USA and BIOCHAIN, Hayward, CA, USA) was amplified in the same way. Aliquots (2.5 μg) of aRNA from individual samples and from the control were reversely transcribed in the presence of Cy5-dCTP and Cy3-dCTP, respectively.

cDNA microarray

Our 'genome-wide' cDNA microarray system contains 27 648 cDNAs selected from the UniGene database of the National Center for Biotechnology Information (32). Fabrication of the microarray, hybridization, washing and detection of signal intensities were described previously (32). To normalize the amount of mRNA between tumors and controls, the Cy5/Cy3 ratio for each gene's expression was adjusted so that the averaged Cy5/Cy3 ratio of 52 housekeeping genes was equal to one. We assigned a cutoff value to each microarray slide using analysis of variance, and the Cy5/Cy3 ratio of the gene was calculated as follows: (1) if Cy5 (cancer sample) was lower than the cutoff level, then the Cy5/Cy3 ratio of the gene was substituted by 2.5 percentile among the Cy5/Cy3 ratios of other genes whose Cy5 and Cy3 were higher than the cutoff level; (2) if Cy3 (control sample) was lower than the cutoff level, then the Cy5/Cy3 ratio of the gene was substituted by 97.5 percentile among the Cy5/Cy3 ratios of other genes whose Cy5 and Cy3 were higher than the cutoff level; (3) if both Cy5 and Cy3 were lower than the cutoff level, then the Cy5/Cy3 ratio of the gene was left blank.

Extraction of genes for predicting responsiveness to gefitinib

To discover genes that might be associated with sensitivity to gefitinib, individual measurements of about 27 648 genes were compared between the two groups of patients, one classified as responders to gefitinib (PR) and the other as non-responders (PD). To reduce the dimensionality of the number of potent genes that could discriminate between the two classes, we extracted only genes that fulfilled two criteria: (1) signal intensities were higher than the cutoff level in at least 60% of either group, and (2) $|MED_{PR} - MED_{PD}| \geq 1$, where MED indicates

the median calculated from log-transformed relative expression ratios in each group. Then random permutation tests were applied to estimate the ability of individual genes to distinguish between the two classes (PR and PD); mean (μ) and standard deviations (σ) were calculated from the log-transformed relative expression ratios of each gene in both groups. A discrimination score (DS) for each gene was defined as follows:

$$\mathrm{DS} = \frac{\mu_{\mathrm{PR}} - \mu_{\mathrm{PD}}}{\sigma_{\mathrm{PR}} + \sigma_{\mathrm{PD}}}$$

The samples were randomly permutated 10 000 times for each pair of groups. Since the DS dataset of each gene showed a normal distribution, we calculated a *P*-value for the user-defined grouping.

Calculation of drug-response scores

We calculated GRS reflecting the expression levels of candidate prediction-genes according to procedures described previously (33,34). Each gene (gi) votes for either responder (PR) or non-responder (PD) depending on whether the expression level (xi) in the sample is closer to the mean expression level of one group or the other in reference samples. The magnitude of the vote (Vi) reflects the deviation of the expression level in the sample from the average of the two classes:

$$\mathrm{Vi} = \left| \mathrm{xi} - \frac{\mu_{\mathrm{PR}} + \mu_{\mathrm{PD}}}{2} \right|$$

We summed the votes to obtain total votes for responders (V_{PR}) and non-responders (V_{PD}), and calculated GRS values as follows:

$$\mathrm{GRS} = \frac{V_{\mathrm{PR}} - V_{PD}}{V_{\mathrm{PR}} + V_{\mathrm{PD}}} \times 100$$

where the GRS value reflects the margin of victory in the direction of either responder or non-responder. GRS values range from -100 to $+100$; the higher an absolute value of GRS, the stronger the prediction.

Cross-validation of scores and evaluation of the prediction system

The prediction scores of all samples were obtained by a leave-one-out approach, in which one sample at a time was removed from the sample set; permutational *P*-values and mean values of the two classes were calculated for each gene using the remaining samples. The drug response of the withheld sample was predicted by calculating the prediction score. These procedures were repeated for each sample (33,34).

To evaluate the reliability of the prediction system, we calculated a 'classification score' (CS) using the GRS values of responders and non-responders in each gene set, as follows (34):

$$\mathrm{CS} = \frac{\mu_{\mathrm{GRSpr}} - \mu_{\mathrm{GRSpd}}}{\sigma_{\mathrm{GRSpr}} + \sigma_{\mathrm{GRSpd}}}$$

A larger value of CS indicates better separation of the two groups by the prediction system.

Hierarchical clustering

We used web-available software ('Cluster' and 'TreeView') written by M. Eisen (http://genome-www5.stanford.edu/MicroArray/SMD/restech.html) to create a graphic representation of the microarray data and to create a dendrogram of hierarchical clustering. Before the clustering algorithm was applied, the fluorescence ratio for each spot was first log-transformed and then the data for each sample were median-centered to remove experimental biases.

Semi-quantitative RT–PCR analysis

Aliquots (5.0 μg) of the same aRNA hybridized to the microarray slides from individual samples and from the normal control lung were reversely transcribed using oligo(dT)$_{12-18}$ primer and SuperScript II reverse transcriptase (Invitrogen, Carlsbad, CA, USA). Semi-quantitative RT–PCR experiments were carried out with the following sets of synthesized primers specific to the 12 top-ranked genes used for establishing a GRS or with beta-actin (*ACTB*)-specific primers as an internal control: *FLJ22662*, 5′-GCCATAAGTGGTCCCACAGT-3′ and 5′-GTCTTCTAGTCCGTCATCTCCCT-3′; Amphiregulin (*AREG*), 5′-CCATAGCTGCCTTTATGTCTGC-3′ and 5′-CTTTTTACCTTCGTGCACCTTT-3′; coronin, actin binding protein, 1C (*CORO1C*), 5′-TAATCTGCTGAGGACCTTTT GTC-3′ and 5′-TAATTCACTGTCCTCTTCTGGGA-3′; apoptosis, caspase activation inhibitor (*AVEN*), 5′-GCTCAC AGCAGTAAATGCCTA-3′ and 5′-TGCTATGCTGTAAAC ACTGGCTA-3′; dual specificity phosphatase 3 (*DUSP3*), 5′-GGATCCTTTATTGGTGGTAGAGC-3′ and 5′-CCAGAG TGACCCTGAAGATAAAT-3′; *DJ473B4*, 5′-ACCTGATTC TCTAGGTGCAGTTT-3′ and 5′-GTCGTTTCAACCAGGT AGTTTTG-3′; pleckstrin homology-like domain, family A, member 2 (*PHLDA2*), 5′-GGGCGCCTTAAGTTATTGG A-3′ and 5′-GGATGGTAGAAAAGCAAACTGG-3′; RNA binding motif protein 7 (*RBM7*), 5′-TGTAATGGAGATTG TACAGGTTG-3′ and 5′-AGGAACAGTACAAATGCTGT GGT-3′; *BX092512* (EST), 5′-GCACTCCTTGAAGGTACA CTAAC-3′ and 5′-ATTTGTATTCACTCAGCCATGC-3′; oncostatin M receptor (*OSMR*), 5′-ACCCAACTTCAAAAC TAGGACTC-3′ and 5′-ACAGCTTGATGTCCTTTCTATGC -3′; glutamate–cysteine ligase, catalytic subunit (*GCLC*), 5′-TCATGAAAGGCACTGAGTTTTG-3′ and 5′-GTTAGC TGAAGCAGCTTTATTGC-3′; collagen, type IV, alpha 3 binding protein (*COL4A3BP*), 5′-ATATGCACAATCCTGG AAGTGA-3′ and 5′-TGCCTTACTAGCATTACCACCAT-3′; *ACTB*, 5′-GAGGTGATAGCATTGCTTTCG-3′ and 5′-CAAG TCAGTGTACAGGTAAGC-3′. PCR reactions were optimized for the number of cycles to ensure product intensity within the logarithmic phase of amplification. We performed phosphorimager quantification analysis (Molecular Imager FX: Bio-Rad Laboratories, Hercules, CA, USA), and RT–PCR band intensities were quantitatively compared with normalized Cy5/Cy3 ratio of gene expression from the microarray data.

Immunohistochemical analysis

To confirm the differential expression of AREG and transforming growth factor-alpha (TGFA) proteins, both of which encode the ligand for EGFR and other ERBB members, and other three candidate markers [a disintegrin and metalloproteinase domain 9 (ADAM9), CD9 antigen (p24) and OSMR], which are also known to relate to the EGFR signaling, for predicting responders versus non-responders to gefitinib, we stained clinical tissue sections obtained by fiberscopic transbronchial biopsy (TBB) and lymph-node biopsy using ENVISION+ Kit/HRP (DakoCytomation). Briefly, after endogenous peroxidase and protein blocking reactions, anti-human AREG polyclonal antibody (Neo Markers, Fremont, CA, USA), anti-human TGFA monoclonal antibody (Calbiochem, Darmstadt, Germany), anti-human ADAM9 monoclonal antibody (R&D Systems Inc. Minneapolis, MN, USA), anti-human CD9 monoclonal antibody (Novocastra Laboratories Ltd, Newcastle upon Tyne, UK) or anti-human OSMR monoclonal antibody (Santa Cruz Biotechnology, Inc., Santa Cruz, CA, USA) was added, and then HRP-labeled anti-rabbit or anti-mouse IgG as the secondary antibody. Substrate chromogen was then added and the specimens were counterstained with hematoxylin.

Frozen tissue samples from 11 patients were selected for analysis of immunohistochemistry. Positivity of immunostaining was assessed semi-quantitatively by scoring intensity as absent or positive by three independent investigators without prior knowledge of the clinical follow-up data. Cases were accepted only as positive if reviewers independently defined them thus.

ELISA

Serum was obtained from an independent set of 35 lung-adenocarcinoma patients who were treated with gefitinib based on the same protocol as this clinical study at Hiroshima University hospital in Japan (five for PR, 10 for SD and 20 for PD). The sera of all the patients were obtained with informed consent at the time of diagnosis and every 4 weeks after the beginning of treatment, and stored at -80°C. The serum TGFA levels were measured by an ELISA using a commercially available enzyme test kits (TGF-alpha ELISA kit: Oncogene Research Products, San Diego, CA, USA).

In vitro gefitinib treatment and AREG-autocrine assay

Human NSCLC (adenocarcinoma) cell lines PC-9, NCI-H358 and NCI-H522 were purchased from the American Type Culture Collection (ATCC; Rockville, MD, USA). To detect expression of *AREG* in these NSCLC cells, total RNA from each line was reverse-transcribed for single-stranded cDNAs using oligo$(dT)_{12-18}$ primer and Superscript II (Invitrogen). Semi-quantitative RT–PCR was carried out as described previously (19). gefitinib [4-(3-chloro-4-fluoroanilino)-7-methoxy-6-(3-morpholinopropoxy) quinazoline: Iressa, ZD1839], an inhibitor of epidermal growth factor receptor tyrosine kinase, was provided by AstraZeneca Pharmaceuticals (Macclesfield, UK). The drug was dissolved in DMSO at a concentration of 10 mM and kept at -20°C.

We performed flow cytometry to determine the sensitivity of lung adenocarcinoma cell lines to gefitinib treatment. Cells were plated at densities of 5×10^5 cells/100 mm dish and treated with 1.0 μM of gefitinib in appropriate serum-free medium. The cells were trypsinized 72 h after the treatment, collected in PBS and fixed in 70% cold ethanol for 30 min. After treatment with 100 μg/ml RNase (Sigma-Aldrich Co., St Louis, MO, USA), the cells were stained with 50 μg/ml propidium iodide (Sigma-Aldrich) in PBS. Flow cytometry was performed on a Becton Dickinson FACScan and analyzed by ModFit software (Verity Software House, Inc., Topsham, ME, USA). The percentages of nuclei in G_0/G_1, S and G_2/M phases of the cell cycle and sub-G1 population were determined from at least 20 000 ungated cells.

To investigate whether AREG functions as an autocrine anti-apoptotic factor in lung adenocarcinoma cells treated with gefitinib, we carried out the following assay. First, gefitinib-sensitive PC-9 cells, which do not express *AREG*, were cultured in serum-free medium for at least 8 h prior to gefitinib treatment. These cells were then incubated with 0.5 or 1.0 μM of gefitinib for 72 h in media that were either serum-free or supplemented with 10% FCS, or in serum-free conditioned medium collected from 72 h cultures of *AREG*-expressing cells (NCI-H358 or NCI-H522). Each medium was replaced once with the same medium containing gefitinib at the 48 h time point. To detect the response of each cell line to gefitinib, viability was evaluated by MTT assays using Cell Counting Kits (WAKO, Osaka, Japan).

To confirm the autocrine effect of AREG on the gefitinib-resistance of NSCLC cells, we cultured PC-9 cells for 72 h in serum-free medium containing 1.0 μM of gefitinib and recombinant AREG protein (Genzyme-Techne, Minneapolis, MN, USA) in final concentrations of 1–100 ng/ml. Cell viability was evaluated by MTT assays. A possible effect of AREG itself on the viability of NSCLC cells was evaluated also, by culturing the PC-9 cells in serum- and gefitinib-free medium containing only recombinant AREG protein. MTT assays were performed as above.

SUPPLEMENTARY MATERIAL

Supplementary Material is available at HMG Online.

ACKNOWLEDGEMENTS

This work was supported in part by a 'Research for the Future' Program Grant of The Japan Society for the Promotion of Science (no. 00L01402) to Y.N. Gefitinib/ZD1839 (sold as Iressa) is produced and provided for this study by AstraZeneca.

REFERENCES

1. Fossella, F.V., DeVore, R., Kerr, R.N., Crawford, J., Natale, R.R., Dunphy, F., Kalman, L., Miller, V., Lee, J.S., Moore, M. *et al.* (2000) Randomized phase III trial of docetaxel versus vinorelbine or ifosfamide in patients with advanced non-small-cell lung cancer previously treated with platinum-containing chemotherapy regimens. The TAX 320 Non-Small Cell Lung Cancer Study Group. *J. Clin. Oncol.*, **18**, 2354–2362.

2. Non-small Cell Lung Cancer Collaborative Group. (1995) Chemotherapy in non-small cell lung cancer: a meta-analysis using updated data on individual patients from 52 randomised clinical trials. *Br. Med. J.*, **311**, 899–909.
3. Schiller, J.H., Harrington, D., Belani, C.P., Langer, C., Sandler, A., Krook, J., Zhu, J. and Johnson, D.H. (2002) Comparison of four chemotherapy regimens for advanced non-small-cell lung cancer. *N. Engl. J. Med.*, **346**, 92–98.
4. Kelly, K., Crowley, J., Bunn, P.A., Jr, Presant, C.A., Grevstad, P.K., Moinpour, C.M., Ramsey, S.D., Wozniak, A.J., Weiss, G.R. and Moore D.F. (2001) Randomized phase III trial of paclitaxel plus carboplatin versus vinorelbine plus cisplatin in the treatment of patients with advanced non-small-cell lung cancer: a Southwest Oncology Group trial. *J. Clin. Oncol.*, **19**, 3210–3218.
5. Baselga, J. (2002) Why the epidermal growth factor receptor? The rationale for cancer therapy. *Oncologist*, **7** (Suppl. 4), 2–8.
6. Traxler, P. (2003) Tyrosine kinases as targets in cancer therapy—successes and failures. *Expert Opin. Ther. Targets*, **7**, 215–234.
7. Wakeling, A.E., Guy, S.P., Woodburn, J.R., Ashton, S.E., Curry, B.J., Barker, A.J. and Gibson, K.H. (2002) ZD1839 (Iressa): an orally active inhibitor of epidermal growth factor signaling with potential for cancer therapy. *Cancer Res.*, **62**, 5749–5754.
8. Herbst, R.S. (2003) Dose-comparative monotherapy trials of ZD1839 in previously treated non-small cell lung cancer patients. *Semin. Oncol.*, **30**, 30–38.
9. Fukuoka, M., Yano, S., Giaccone, G., Tamura, T., Nakagawa, K., Douillard, J.Y., Nishiwaki, Y., Vansteenkiste, J., Kudoh, S., Rischin, D. *et al.* (2003) Multi-institutional randomized phase II trial of gefitinib for previously treated patients with advanced non-small-cell lung cancer. *J. Clin. Oncol.*, **21**, 2237–2246.
10. Kris, M.G., Natale, R.B., Herbst, R.S., Lynch, T.J. Jr, Prager. D., Belani, C.P., Schiller, J.H., Kelly, K., Spiridonidis, H., Sandler, A. *et al.* (2003) Efficacy of gefitinib, an inhibitor of the epidermal growth factor receptor tyrosine kinase, in symptomatic patients with non-small cell lung cancer: a randomized trial. *J. Am. Med. Assoc.*, **290**, 2149–2158.
11. Inoue, A., Saijo, Y., Maemondo, M., Gomi, K., Tokue, Y., Kimura, Y., Ebina, M., Kikuchi, T., Moriya, T. and Nukiwa, T. (2003) Severe acute interstitial pneumonia and gefitinib. *Lancet*, **361**, 137–139.
12. Miller, V.A., Kris, M.G., Shah, N., Patel, J., Azzoli, C., Gomez, J., Krug, L.M., Pao, W., Rizvi, N., Pizzo, B. *et al.* (2004) Bronchioloalveolar pathologic subtype and smoking history predict sensitivity to gefitinib in advanced non-small-cell lung cancer. *J. Clin. Oncol.*, **22**, 1103–1109.
13. Ebright, M.I., Zakowski, M.F., Martin, J., Venkatraman, E.S., Miller, V.A., Bains, M.S., Downey, R.J., Korst, R.J., Kris, M.G. and Rusch, V.W. (2002) Clinical pattern and pathologic stage but not histologic features predict outcome for bronchioloalveolar carcinoma. *Ann. Thorac. Surg.*, **74**, 1640–1646.
14. Paez, J.G., Janne, P.A., Lee, J.C., Tracy, S., Greulich, H., Gabriel, S., Herman, P., Kaye, F.J., Lindeman, N., Boggon, T.J. *et al.* (2004) EGFR mutations in lung cancer: correlation with clinical response to gefitinib therapy. *Science*, **304**, 1497–1500.
15. Lynch, T.J., Bell, D.W., Sordella, R., Gurubhagavatula, S., Okimoto, R.A., Brannigan, B.W., Harris, P.L., Haserlat, S.M., Supko, J.G., Haluska, F.G. *et al.* (2004) Activating mutations in the epidermal growth factor receptor underlying responsiveness of non-small-cell lung cancer to gefitinib. *N. Engl. J. Med.*, **350**, 2129–2139.
16. Sordella, R., Bell, D.W., Haber, D.A. and Settleman, J. (2004) Gefitinib-sensitizing EGFR mutations in lung cancer activate anti-apoptotic pathways. *Science*, **305**, 1163–1167.
17. Kikuchi, T., Daigo, Y., Katagiri, T., Tsunoda, T., Okada, K., Kakiuchi, S., Zembutsu, H., Furukawa, Y., Kawamura, M., Kobayashi, K. *et al.* (2003) Expression profiles of non-small cell lung cancers on cDNA microarrays: identification of genes for prediction of lymph-node metastasis and sensitivity to anti-cancer drugs. *Oncogene*, **22**, 2192–2205.
18. Beer, D.G., Kardia, S.L., Huang, C.C., Giordano, T.J., Levin, A.M., Misek, D.E., Lin, L., Chen, G., Gharib, T.G., Thomas, D.G. *et al.* (2002) Gene-expression profiles predict survival of patients with lung adenocarcinoma. *Nat. Med.*, **8**, 816–824.
19. Zembutsu. H., Ohnishi, Y., Daigo, Y., Katagiri, T., Kikuchi, T., Kakiuchi, S., Nishime, C., Hirata, K. and Nakamura, Y. (2003) Gene-expression profiles of human tumor xenografts in nude mice treated orally with the EGFR tyrosine kinase inhibitor ZD1839. *Int. J. Oncol.*, **23**, 29–39.
20. Fontanini, G., De Laurentiis, M., Vignati, S., Chine, S., Lucchi, M., Silvestri, V., Mussi, A., De Placido, S., Tortora, G., Bianco, A.R. *et al.* (1998) Evaluation of epidermal growth factor-related growth factors and receptors and of neoangiogenesis in completely resected stage I–IIIA non-small-cell lung cancer: amphiregulin and microvessel count are independent prognostic indicators of survival. *Clin. Cancer Res.*, **4**, 241–249.
21. Hurbin, A., Dubrez, L., Coll, J.L. and Favrot, M.C. (2002) Inhibition of apoptosis by amphiregulin via an insulin-like growth factor-1 receptor-dependent pathway in non-small cell lung cancer cell lines. *J. Biol. Chem.*, **277**, 49127–49133.
22. Yarden, Y. and Sliwkowski, M.X. (2001) Untangling the ErbB signalling network. *Nat. Rev. Mol. Cell. Biol.*, **2**, 127–137.
23. Zhou, B., Wang, Z.X., Zhao, Y., Brautigan, D.L. and Zhang, Z.Y. (2002) The specificity of extracellular signal-regulated kinase 2 dephosphorylation by protein phosphatases. *J. Biol. Chem.*, **277**, 31818–31825.
24. Prenzel, N., Zwick, E., Daub, H., Leserer, M., Abraham, R., Wallasch, C. and Ullrich, A. (1999) EGF receptor transactivation by G-protein-coupled receptors requires metalloproteinase cleavage of proHB-EGF. *Nature*, **402**, 884–888.
25. Shi, W., Fan, H., Shum, L. and Derynck R. (2000) The tetraspanin CD9 associates with transmembrane TGF-alpha and regulates TGF-alpha-induced EGF receptor activation and cell proliferation. *J. Cell. Biol.*, **148**, 591–602.
26. Grant, S.L., Hammacher, A., Douglas, A.M., Goss, G.A., Mansfield, R.K., Heath, J.K. and Begley, C.G. (2002) An unexpected biochemical and functional interaction between gp130 and the EGF receptor family in breast cancer cells. *Oncogene*, **21**, 460–474.
27. Chau, B.N., Cheng, E.H., Kerr, D.A. and Hardwick, J.M. (2000) Aven, a novel inhibitor of caspase activation, binds Bcl-xL and Apaf-1. *Mol. Cell*, **6**, 31–41.
28. Tipnis, S.R., Blake, D.G., Shepherd, A.G. and McLellan, L.I. (1999) Overexpression of the regulatory subunit of *R*-glutamylcysteine synthetase in Hela cells increases *R*-glutamylcysteine synthetase activity and confers drug resistance. *Biochem. J.*, **337**, 559–566.
29. Hedenfalk, I., Duggan, D., Chen, Y., Radmacher, M., Bittner, M., Simon, R., Meltzer, P., Gusterson, B., Esteller, M., Kallioniemi, O.P. *et al.* (2001) Gene-expression profiles in hereditary breast cancer. *N. Engl. J. Med.*, **344**, 539–548.
30. Hofmann, W.K., de Vos, S., Elashoff, D., Gschaidmeier, H., Hoelzer, D., Koeffler, H.P. and Ottmann, O.G. (2002) Relation between resistance of Philadelphia-chromosome-positive acute lymphoblastic leukaemia to the tyrosine kinase inhibitor STI571 and gene-expression profiles: a gene-expression study. *Lancet*, **359**, 481–486.
31. Bohm, M., Wieland, I., Schutze, K. and Rubben, H. (1997) Microbeam MOMeNT: non-contact laser microdissection of membrane-mounted native tissue. *Am. J. Pathol.*, **151**, 63–67.
32. Kakiuchi, S., Daigo, Y., Tsunoda, T., Yano, S., Sone, S. and Nakamura, Y. (2003) Genome-wide analysis of organ-preferential metastasis of human small cell lung cancer in mice. *Mol. Cancer Res.*, **1**, 485–499.
33. Golub, T.R., Slonim, D.K., Tamayo, P., Huard, C., Gaasenbeek, M., Mesirov, J.P., Coller, H., Loh, M.L., Downing, J.R., Caligiuri, M.A. *et al.* (1999) Molecular classification of cancer: class discovery and class prediction by gene expression monitoring. *Science*, **286**, 531–537.
34. Ochi, K., Daigo, Y., Katagiri, T., Nagayama, S., Tsunoda, T., Myoui, A., Naka, N., Araki, N., Kudawara, I., Ieguchi, M. *et al.* (2004) Prediction of response to neoadjuvant chemotherapy for osteosarcoma by gene-expression profiles. *Int. J. Oncol.*, **24**, 647–655.